ISSN 1070-3284, Russian Journal of Coordination Chemistry, 2007, Vol. 33, No. 4, pp. 233–243. © Pleiades Publishing, Ltd., 2007.
Original Russian Text © A.V. Ivanov, A.S. Zaeva, E.V. Novikova, A.V. Gerasimenko, W. Forsling, 2007, published in Koordinatsionnaya Khimiya, 2007, Vol. 33, No. 4, pp. 243–253.

Adducts of Zinc and Copper(II) Dialkyldithiocarbamate Complexes with Dibutyl- and Diisobutylamines: Synthesis, Structures, EPR and Solid-State Natural Abundance ^{13}C and ^{15}N CP/MAS NMR Spectra

A. V. Ivanov[a], A. S. Zaeva[a,b], E. V. Novikova[a,b], A. V. Gerasimenko[c], and W. Forsling[d]

[a] *Institute of Geology and Nature Management, Amur Scientific Center, Far East Division,*
Russian Academy of Sciences, Ryolochyi per. 1, Blagoveshchensk, Russia
[b] *Blagoveshchensk State Pedagogical University, Blagoveshchensk, 675000 Russia*
[c] *Institute of Chemistry, Far East Division, Russian Academy of Sciences,*
pr. Stoletiya Vladivostoka 159, Vladivostok, 690022 Russia
[d] *Luléa University of Technology, S-971 87, Luléa, Sweden*

Received April 3, 2006

Abstract—Crystalline adducts of zinc and copper(II) dithiocarbamate complexes with dibutyl- and diisobutylamines of the general formula $[M(NHR'_2)(S_2CNR_2)_2]$ (M = Zn, ^{63}Cu, and ^{65}Cu; R = CH_3 and C_2H_5; $R_2 = (CH_2)_4O$; R' = C_4H_9 and *i*-C_4H_9) were synthesized. Their structures and spectroscopic properties were studied by EPR and solid-state natural abundance ^{13}C and ^{15}N CP/MAS NMR spectroscopy. Experimental EPR data and computer-assisted modeling confirmed the individual character of copper(II) adducts. The geometries of the copper coordination polyhedra were found to be intermediate between a tetragonal pyramid and a trigonal bipyramid (TBP). The contributions from TBP to the geometries of the adducts obtained were calculated from the EPR data. According to the X-ray diffraction data, the adduct of zinc diethyldithiocarbamate with diisobutylamine exists in two isomeric forms. The ^{13}C and ^{15}N CP/MAS NMR signals were assigned to the atomic positions in two crystallographically independent conformer molecules.

DOI: 10.1134/S107032840704001X

Dithiocarbamates of many metals tend to reversibly add organic N-, O-, S-, and P-donor bases to give heteroligand complexes generically called adducts. Because their molecules are usually highly volatile in vacuum, such adducts are of practical interest as technological precursors of metal-sulfide films with semiconducting and luminescent properties [1]. Earlier, conformational isomerism of adducts with both planar [2–5] and nonplanar cyclic N-donor bases [6, 7] has been found in crystalline adducts of zinc and copper(II) dithiocarbamates (**Dtcs**) with pyridine and morpholine.

In this study, we obtained adducts of zinc and copper(II) dimethyl- and diethyldithiocarbamates and their morpholine analogs with dibutyl- and diisobutylamines of the general formula $[M(NHR'_2)(S_2CNR_2)_2]$ (M = Zn, ^{63}Cu, and ^{65}Cu; R = CH_3 and C_2H_5; $R_2 = (CH_2)_4O$; R' = C_4H_9 and i–C_4H_9) and performed their detailed characterization by EPR and solid-state ^{13}C and ^{15}N MAS NMR spectroscopy. We discovered conformational isomerism in adducts with acyclic N-donor bases. The signals in the ^{13}C and ^{15}N MAS NMR spectra of the adducts were assigned to the atomic positions in two crystallographically independent conformers of $[Zn\{NH(i\text{-}C_4H_9)_2\}\{S_2CN(C_2H_5)_2\}_2]$.

EXPERIMENTAL

The starting binuclear zinc dimethyl- and diethyl- and morpholinedithiocarbamates of the general formula $[Zn_2(S_2CNR_2)_4]$ (R = CH_3 and C_2H_5 or $R_2 = (CH_2)_4O$) were prepared by reactions of Zn^{2+} with appropriate dithiocarbamate ions in aqueous solutions [8]. The resulting bulky precipitates were washed by decantation, filtered off, and dried in air.

(Dibutylamine)bis(dimethyldithiocarbamato)zinc $[Zn\{NH(C_4H_9)_2\}\{S_2CN(CH_3)_2\}_2]$ (**I**), (dibutylamine)bis(diethyldithiocarbamato)zinc $[Zn\{NH(C_4H_9)_2\}\{S_2CN(C_2H_5)_2\}_2]$ (**II**), (dibutylamine)bis(morpholinedithiocarbamato)zinc $[Zn\{NH(C_4H_9)_2\}\{S_2CN(CH_2)_4O\}_2]$ (**III**), (diisobutylamine)bis(dimethyldithiocarbamato)zinc $[Zn\{NH(i\text{-}C_4H_9)_2\}\{S_2CN(CH_3)_2\}_2]$ (**IV**), and bis(diethyldithiocarbamato)(diisobutylamine)zinc $[Zn\{NH(i\text{-}C_4H_9)_2\}\{S_2CN(C_2H_5)_2\}_2]$ (**V**) were synthesized in two ways: (1) by reactions of binuclear zinc complexes with dialkylamines in toluene followed by room-temperature crystallization of adducts and (2) by quantitative absorption of the dialkylamine vapor from the gas phase by powdered binuclear zinc complexes. The degrees of conversion of the starting complexes into adducts were checked by ^{13}C NMR spectroscopy and gravimetry.

For adducts **I**–**V** obtained by crystallization from toluene, elemental analysis[1] for zinc gave the following results:

For $ZnS_4N_3C_{14}H_{31}$ (I), $M = 435.07$
anal. calcd. (wt %): Zn, 15.03.
Found, (wt %): Zn, 15.03/15.22 (for the ^{64}Zn/^{66}Zn nuclides).
For $ZnS_4N_3C_{18}H_{39}$ (II), $M = 491.13$
anal. calcd. (wt %): Zn, 13.31.
Found, (wt %): Zn, 13.10/13.04.
For $ZnS_4O_2N_3C_{18}H_{35}$ (III) $M = 519.14$
anal. calcd. (wt %): Zn, 12.60.
Found, (wt %): Zn, 12.53/12.64.
For $ZnS_4N_3C_{14}H_{31}$ (IV), $M = 435.07$
anal. calcd. (wt %): Zn, 15.03.
Found, (wt %): Zn, 14.39/14.83.
For $ZnS_4N_3C_{18}H_{39}$ (V), $M = 491.13$
anal. calcd. (wt %): Zn, 13.31.
Found, (wt %): Zn, 13.28/13.39.

Single crystals of V for X-ray diffraction analysis were grown from a solution in toluene.

(Dibutylamine)bis(dimethyldithiocarbamato)copper(II) $[Cu\{NH(C_4H_9)_2\}\{S_2CN(CH_3)_2\}_2]$ (**VI**), (dibutylamine)bis(diethyldithiocarbamato)copper(II) $[Cu\{NH(C_4H_9)_2\}\{S_2CN(C_2H_5)_2\}_2]$ (**VII**), (dibutylamine)bis(morpholinedithiocarboamato)copper(II) $[Cu\{NH(C_4H_9)_2\}\{S_2CN(CH_2)_4O\}_2]$ (**VIII**), (diisobutylamine)bis(dimethyldithiocarbamato)copper(II) $[Cu\{NH(i\text{-}C_4H_9)_2\}\{S_2CN(CH_3)_2\}_2]$ (**IX**), and bis(diethyldithiocarbamato)(diisobutylamine)copper(II) $[Cu\{NH(i\text{-}C_4H_9)_2\}\{S_2CN(C_2H_5)_2\}_2]$ (**X**) were obtained as described for adducts **I**–**V** from isotope-substituted cupric salts magnetically diluted with zinc (Cu : Zn = 1 : 1000; Cu, 99.3(1) and 99.2(1) at % for ^{63}Cu and ^{65}Cu, respectively). This was done to enhance the resolution of EPR spectra. The degrees of conversion of the starting complexes into adducts were checked by gravimetry and EPR spectroscopy. All the adducts obtained were stored in sealed tubes.

The EPR spectra of magnetically diluted complexes **VI**–**X** were recorded on a 70-02 XD/1 radio spectrometer (~9.5 GHz; MP SZ, Minsk) at ~295 K. The operating frequency was measured with a ChZ-46 microwave frequency meter. *g* Factors were calculated with reference to DPPH. The error in the determination of *g* factors was ±0.002; the constants of the hyperfine structure (HFS) are quoted in oersteds (Oe) to within ±2%. EPR spectra were modeled at the MP2 level with the WIN-EPR SimFonia program (Bruker Co. software, version 1.2). *g* Factors, HFS constants, resonance line widths, and percent contributions from the Lorentz and Gauss components to the line shape were variables in the modeling.

^{13}C and ^{15}N MAS NMR spectra were recorded on a CMX-360 pulse spectrometer (Chemagnetics Infinity) operating at 90.52 and 36.48 MHz, respectively (superconducting magnet with $B_0 = 8.46$ T; Fourier transform). The ^{13}C–^{1}H and ^{15}N–^{1}H cross polarization techniques were used; ^{13}C/^{15}N and ^{15}N–^{1}H dipolar interactions were suppressed via proton decoupling in a magnetic field with the corresponding proton resonance frequency [9]. Samples (~350 mg) of the adducts were packed into ZrO_2 rotors (7.5 mm in diameter). The spinning frequences in ^{13}C/^{15}N MAS NMR experiments were 5000/2800–3000(1) Hz, respectively. The numbers of scans were 400–2400/3080–7600. The proton $\pi/2$ pulse durations were 4.5/5.0 μs. The ^{1}H–^{13}C/^{1}H–^{15}N contact times were 2.0/1.25–2.5 ms; the excitation pulses were spaced at 2.0/2.5 s.

Isotropic ^{13}C and ^{15}N chemical shifts δ (ppm) are referenced to a line of crystalline adamantane used as the external standard (δ = 38.56 ppm relative to tetramethylsilane [10]) and crystalline NH_4Cl (δ 0 ppm; –341 ppm on the absolute scale [11, 12]), respectively. The width of the reference line at δ 38.56 ppm (2.6 Hz) for crystalline adamantane was used to check the homogeneity of the magnetic field. The δ values were corrected for drift of the magnetic field strength during the measurements (its frequency equivalents for the ^{13}C/^{15}N nuclei were 0.050/0.017 Hz/h). The chemical shifts and the integrated intensity ratios for the overlapping signals were additionally refined by fragment-by-fragment mathematical modeling of the spectra with consideration of the line positions and widths and the contributions from the Lorentz and Gauss components to the line shapes.

X-ray diffraction analysis of complex **V** was performed on a SMART 1000 CCD diffractometer (MoK_α radiation, graphite monochromator) for an edged single crystal. Reflections were collected in the hemisphere [13] (crystal–detector distance 50 mm, ω scan mode, scan step 0.2°, frame exposure time 10 s). Absorption correction was applied from equivalent reflections. The structure was solved by the direct method and refined by the least-squares method in the anisotropic approximation for non-hydrogen atoms. The hydrogen atoms were located geometrically and refined in the rider model. The collected data were edited and the unit cell parameters were refined with the SMART and SAINT-Plus programs [13]. All calculations for structure deter-

---

[1] Elemental analysis was carried out by high-resolution mass spectrometry with inductively coupled plasma (HR-ICP-MS) in the medium-resolution range, $\Delta m/m \approx 4500$ (ELEMENT, Finnigan MAT, Bremen, Germany).

mination and refinement were performed with the SHELXTL/PC programs [14]. Selected crystallographic parameters and a summary of data collection and refinement are summarized in Table 1. Atomic coordinates are listed in Table 2. Bond lengths and angles are given in Table 3.

RESULTS AND DISCUSSION

EPR spectra. A comparative analysis of the experimental and model EPR spectra of magnetically diluted isotope-substituted copper(II) adducts **VI**–**X** revealed their spectral individualities, although they show a number of signs in common (Figs. 1, 2; Table 4): triaxial anisotropy of the g and A^{Cu} tensors (provided the orientation with $g_3 \approx 2.00$), the presence of quartets of the resolved HFS due to ^{63}Cu or ^{65}Cu nuclei ($I = 3/2$) in all the three orientations, and the presence of an intense peak of extra absorption (**EA**) in the high-field range [15, 16] (the spectrum of complex **IX** shows two AA peaks). This character of anisotropy suggests that the coordination polyhedra of the copper atom (C.N. 5) are intermediate between a tetragonal pyramid (**TP**) and a trigonal bipyramid (**TBP**) and that the ground state of the unpaired electron results from mixing of the $3d_{x^2-y^2}$- and $3d_{z^2}$-AO of copper(II) [17, 18].

Contributions from TP and TBP to the geometries of the copper polyhedra were quantitatively estimated in terms of a methodological approach involving the parameter $\Delta = A_1^{Cu} - A_2^{Cu}$ [19]. For some adducts, we have found a correlation between the parameter Δ and the contribution from TBP to the geometry of the copper polyhedron. For instance, with an increase in that contribution from 55 to 85%, the parameter Δ linearly decreases from 105 to 64 Oe.

The copper(II) adducts obtained can be arranged in the following order of increasing contribution from TBP: **VIII**, **X**, **IX**, **VI**, and **VII** with Δ = 114, 89, 77, 42, and 26 Oe, respectively. Therefore, the contributions from TBP are $\leqslant$ 55% for **VIII**, > 60% for **X,** ~75% for **IX**, and > 85% for **VI** and **VII**.

^{13}C and ^{15}N MAS NMR spectra. A comparison of the ^{13}C and ^{15}N MAS NMR spectra of the starting binuclear zinc dithiocarbamates and adducts **I–V** revealed that adduct formation is always accompanied by dissociation of binuclear molecules. The individuality of each complex was evident from their experimental NMR spectra. The ^{13}C NMR spectra of crystalline adducts **I**–**V** (Fig. 3; Table 5) show signals for =NC(S)S–fragments and signals for alkyl (alkoxy) substituents in the Dtc ligands and coordinated bases. The range in which Dtc fragments resonate is most informative. In this range, the ^{13}C NMR spectra of adducts **I–III** exhibit two (1 : 1) signals (Table 5) for two structurally nonequivalent Dtc fragments. For adducts **I** and **II**, these signals are asymmetric 1 : 2 doublets arising from a coupling of the ^{13}C nucleus with the quadrupole

Table 1. Selected crystallographic parameters and a summary of data collection and refinement for $[Zn\{NH(i\text{-}C_4H_9)_2\}\{S_2CN(C_2H_5)_2\}_2]$ (V)

Parameter	Value
M	491.13
T, K	173(1)
λ, Å	0.71073
Crystal system	Monoclinic
Space group	$P2_1/c$
a, Å	16.534(2)
b, Å	26.691(3)
c, Å	11.403(1)
β, deg	91.540(2)
V, Å^3	5030.4(9)
Z	8
ρ_{calcd}, g/cm^3	1.297
μ, mm^{-1}	1.317
F(000)	2096
Crystal shape (size, mm)	Prism (0.30 × 0.24 × 0.16)
θ scan range, deg	3.78–28.03
Ranges of h, k, and l indices	$-21 \le h \le 21$, $-35 \le k \le 32$, $-15 \le l \le 12$
Number of measured reflections	30684
Number of independent reflections	12007 (R_{int} = 0.0449)
Number of reflections with $I > 2\sigma(I)$	8805
Refinement method	Full-matrix least squares on F^2
Number of parameters refined	491
GOOF	1.012
R factors for $F^2 > 2\sigma(F^2)$	R_1 = 0.0372, wR_2 = 0.0786
R factors for all reflections	R_1 = 0.0624, wR_2 = 0.0879
Extinction coefficient	not refined
Residual electron density (min/max), e/Å^3	–0.359/0.616

Table 2. Atomic coordinates ($\times 10^4$) and isotropic equivalent thermal parameters U_{equiv} for complex $[\text{Zn}\{\text{NH}(i\text{-C}_4\text{H}_9)_2\}\{\text{S}_2\text{CN}(\text{C}_2\text{H}_5)_2\}_2]$V

Atom	*x*	*y*	*z*	U_{equiv}, Å^2	Atom	*x*	*y*	*z*	U_{equiv}, Å^2
Zn(1)	1416.3(2)	6043.5(1)	4881.8(2)	0.02348(7)	C(11)	790(2)	6928(1)	3408(2)	0.0322(6)
Zn(2)	3661.4(2)	3752.9(1)	9688.2(2)	0.02324(7)	C(12)	–77(2)	6806(1)	3647(3)	0.0425(7)
S(1)	1438.8(3)	6449.5(2)	7157.1(5)	0.0290(1)	C(13)	–378(2)	7076(1)	4731(3)	0.0573(9)
S(2)	313.0(3)	5757.3(2)	5886.8(5)	0.0241(1)	C(14)	–602(2)	6948(1)	2561(3)	0.069(1)
S(3)	2747.2(3)	5737.4(2)	4844.5(5)	0.0244(1)	C(15)	2170(1)	7012(1)	4259(2)	0.0285(5)
S(4)	1475.2(3)	5572.3(2)	3018.4(5)	0.0284(1)	C(16)	2233(2)	7574(1)	4375(2)	0.0336(6)
S(5)	2255.9(3)	3892.3(2)	9535.8(5)	0.0250(1)	C(17)	3095(2)	7733(1)	4110(3)	0.0478(8)
S(6)	3372.4(3)	4159.4(2)	7654.0(5)	0.0274(1)	C(18)	1999(2)	7746(1)	5582(3)	0.0532(8)
S(7)	4012.4(4)	3484.8(2)	11806.7(5)	0.0279(1)	C(19)	2413(1)	4175(1)	8185(2)	0.0201(5)
S(8)	4650.5(3)	4319.2(2)	10408.4(5)	0.0254(1)	C(20)	980(1)	4420(1)	8029(2)	0.0318(6)
N(1)	25(1)	6150(1)	7977(2)	0.0243(4)	C(21)	830(2)	4894(1)	8715(3)	0.0433(7)
N(2)	2955(1)	5168(1)	2960(2)	0.0244(4)	C(22)	1935(2)	4664(1)	6481(2)	0.0288(5)
N(3)	1344(1)	6795(1)	4396(2)	0.0228(4)	C(23)	1834(2)	4315(1)	5433(2)	0.0399(7)
N(4)	1810(1)	4400(1)	7597(2)	0.0234(4)	C(24)	4700(1)	3966(1)	11677(2)	0.0210(5)
N(5)	5246(1)	4069(1)	12522(2)	0.0224(4)	C(25)	5826(1)	4484(1)	12420(2)	0.0291(5)
N(6)	4161(1)	3110(1)	8926(2)	0.0227(4)	C(26)	6629(2)	4322(1)	11951(2)	0.0358(6)
C(1)	545(1)	6128(1)	7101(2)	0.0220(5)	C(27)	5328(1)	3755(1)	13585(2)	0.0263(5)
C(2)	–779(1)	5909(1)	7916(2)	0.0293(5)	C(28)	5835(2)	3291(1)	13416(2)	0.0364(6)
C(3)	–1422(2)	6272(1)	7470(3)	0.0386(6)	C(29)	3950(1)	2615(1)	9436(2)	0.0282(5)
C(4)	204(2)	6438(1)	9053(2)	0.0331(6)	C(30)	3052(1)	2517(1)	9484(2)	0.0311(6)
C(5)	681(2)	6131(1)	9948(2)	0.0435(7)	C(31)	2637(2)	2556(1)	8282(3)	0.0468(8)
C(6)	2447(1)	5459(1)	3532(2)	0.0216(5)	C(32)	2923(2)	1992(1)	9999(3)	0.0481(8)
C(7)	2714(2)	4902(1)	1871(2)	0.0290(5)	C(33)	5059(1)	3152(1)	8871(2)	0.0265(5)
C(8)	2892(2)	5204(1)	784(2)	0.0378(6)	C(34)	5351(1)	3529(1)	7974(2)	0.0272(5)
C(9)	3795(1)	5090(1)	3372(2)	0.0308(6)	C(35)	5125(2)	3376(1)	6725(2)	0.0475(7)
C(10)	3875(2)	4661(1)	4241(2)	0.0401(7)	C(36)	6271(2)	3569(1)	8133(3)	0.0415(7)

Table 3. Selected bond lengths, bond angles ω, and torsion angles φ in the conformers of complex $[Zn\{NH(i\text{-}C_4H_9)_2\}\{S_2CN(C_2H_5)_2\}_2]$

Bond	*d*, Å	Bond	*d*, Å	Bond	*d*, Å	Bond	*d*, Å
Conformer A		Conformer B		Conformer A		Conformer B	
Zn(1)–N(3)	2.084(2)	Zn(2)–N(6)	2.104(2)	C(4)–C(5)	1.514(4)	C(27)–C(28)	1.510(3)
Zn(1)–S(1)	2.8110(7)	Zn(2)–S(7)	2.5707(7)	N(2)–C(7)	1.476(3)	N(4)–C(22)	1.474(3)
Zn(1)–S(2)	2.3101(6)	Zn(2)–S(8)	2.3582(7)	N(2)–C(9)	1.468(3)	N(4)–C(20)	1.471(3)
Zn(1)–S(3)	2.3490(6)	Zn(2)–S(5)	2.3553(7)	C(7)–C(8)	1.514(3)	C(22)–C(23)	1.521(4)
Zn(1)–S(4)	2.4733(7)	Zn(2)–S(6)	2.5937(7)	C(9)–C(10)	1.517(4)	C(20)–C(21)	1.511(4)
S(1)–C(1)	1.710(2)	S(7)–C(24)	1.723(2)	N(3)–C(11)	1.476(3)	N(6)–C(33)	1.493(3)
S(2)–C(1)	1.736(2)	S(8)–C(24)	1.727(2)	N(3)–C(15)	1.495(3)	N(6)–C(29)	1.488(3)
S(3)–C(6)	1.732(2)	S(5)–C(19)	1.741(2)	C(11)–C(12)	1.502(4)	C(33)–C(34)	1.521(3)
S(4)–C(6)	1.722(2)	S(6)–C(19)	1.713(2)	C(12)–C(13)	1.526(4)	C(34)–C(36)	1.530(3)
N(1)–C(1)	1.336(3)	N(5)–C(24)	1.332(3)	C(12)–C(14)	1.540(4)	C(34)–C(35)	1.519(4)
N(2)–C(6)	1.328(3)	N(4)–C(19)	1.329(3)	C(15)–C(16)	1.510(3)	C(29)–C(30)	1.511(3)
N(1)–C(2)	1.477(3)	N(5)–C(25)	1.472(3)	C(16)–C(17)	1.526(3)	C(30)–C(31)	1.520(4)
N(1)–C(4)	1.471(3)	N(5)–C(27)	1.477(3)	C(16)–C(18)	1.511(4)	C(30)–C(32)	1.536(3)
C(2)–C(3)	1.516(3)	C(25)–C(26)	1.507(3)				
Angle	ω, deg	Angle	ω, deg	Angle	ω, deg	Angle	ω, deg
N(3)Zn(1)S(1)	82.72(6)	N(6)Zn(2)S(7)	94.60(6)	C(9)N(2)C(7)	115.7(2)	C(20)N(4)C(22)	115.1(2)
N(3)Zn(1)S(2)	114.19(5)	N(6)Zn(2)S(8)	113.01(5)	N(1)C(1)S(1)	121.5(2)	N(5)C(24)S(7)	121.8(2)
N(3)Zn(1)S(3)	112.16(5)	N(6)Zn(2)S(5)	119.73(5)	N(1)C(1)S(2)	119.3(2)	N(5)C(24)S(8)	120.6(2)
N(3)Zn(1)S(4)	105.35(6)	N(6)Zn(2)S(6)	92.10(6)	N(1)C(2)C(3)	111.1(2)	N(5)C(25)C(26)	113.2(2)
S(2)Zn(1)S(1)	70.16(2)	S(8)Zn(2)S(7)	73.39(2)	N(1)C(4)C(5)	111.6(2)	N(5)C(27)C(28)	113.5(2)
S(3)Zn(1)S(4)	75.46(2)	S(5)Zn(2)S(6)	73.15(2)	N(2)C(6)S(4)	122.2(2)	N(4)C(19)S(6)	121.4(2)
S(1)Zn(1)S(4)	171.53(2)	S(7)Zn(2)S(6)	171.24(2)	N(2)C(6)S(3)	120.3(2)	N(4)C(19)S(5)	120.9(2)
S(2)Zn(1)S(3)	130.28(2)	S(8)Zn(2)S(5)	126.73(2)	N(2)C(7)C(8)	112.3(2)	N(4)C(22)C(23)	111.7(2)
S(1)Zn(1)S(3)	99.30(2)	S(7)Zn(2)S(5)	108.10(2)	N(2)C(9)C(10)	112.4(2)	N(4)C(20)C(21)	111.9(2)
S(4)Zn(1)S(2)	107.93(2)	S(6)Zn(2)S(8)	98.78(2)	C(11)N(3)C(15)	112.2(2)	C(29)N(6)C(33)	109.1(2)
C(1)S(1)Zn(1)	77.40(8)	C(24)S(7)Zn(2)	81.07(8)	C(11)N(3)Zn(1)	117.6(2)	C(29)N(6)Zn(2)	117.6(1)
C(1)S(2)Zn(1)	92.71(8)	C(24)S(8)Zn(2)	87.59(8)	N(3)C(11)C(12)	112.7(2)	N(6)C(33)C(34)	114.3(2)
C(6)S(3)Zn(1)	85.31(7)	C(19)S(5)Zn(2)	87.88(7)	C(11)C(12)C(13)	112.2(2)	C(33)C(34)C(36)	107.4(2)
C(6)S(4)Zn(1)	81.70(8)	C(19)S(6)Zn(2)	81.02(8)	C(11)C(12)C(14)	108.7(3)	C(33)C(34)C(35)	112.3(2)
S(1)C(1)S(2)	119.2(1)	S(7)C(24)S(8)	117.6(1)	C(13)C(12)C(14)	110.3(3)	C(35)C(34)C(36)	110.4(2)
S(4)C(6)S(3)	117.5(1)	S(6)C(19)S(5)	117.7(1)	C(15)N(3)Zn(1)	110.7(1)	C(33)N(6)Zn(2)	110.9(1)
C(1)N(1)C(4)	121.9(2)	C(24)N(5)C(27)	121.5(2)	N(3)C(15)C(16)	115.8(2)	N(6)C(29)C(30)	114.1(2)
C(1)N(1)C(2)	122.8(2)	C(24)N(5)C(25)	121.9(2)	C(15)C(16)C(17)	108.8(2)	C(29)C(30)C(31)	112.1(2)
C(4)N(1)C(2)	115.3(2)	C(25)N(5)C(27)	116.5(2)	C(15)C(16)C(18)	111.3(2)	C(29)C(30)C(32)	108.5(2)
C(6)N(2)C(7)	122.3(2)	C(19)N(4)C(22)	122.1(2)	C(18)C(16)C(17)	111.0(2)	C(31)C(30)C(32)	110.1(2)
C(6)N(2)C(9)	122.1(2)	C(19)N(4)C(20)	122.8(2)				
Angle	φ, deg	Angle	φ, deg	Angle	φ, deg	Angle	φ, deg
Zn(1)S(3)S(4)C(6)	–176.8(1)	Zn(2)S(7)S(8)C(24)	–172.7(1)	S(4)C(6)N(2)C(7)	–2.8(3)	S(6)C(19)N(4)C(22)	–2.5(3)
Zn(1)S(1)S(2)C(1)	–171.5(2)	Zn(2)S(5)S(6)C(19)	–173.7(1)	S(4)C(6)N(2)C(9)	177.2(2)	S(6)C(19)N(4)C(20)	–180.0(2)
S(3)ё(6)Zn(1)S(4)	177.3(1)	S(8)C(24)Zn(2)S(7)	–173.9(1)	S(1)Zn(1)N(3)C(11)	–139.0(2)	S(6)Zn(2)N(6)C(29)	–138.7(2)
S(1)ё(1)Zn(1)S(2)	172.9(1)	S(5)C(19)Zn(2)S(6)	174.7(1)	S(1)Zn(1)N(3)C(15)	90.2(2)	S(6)Zn(2)N(6)C(33)	94.8(1)
S(1)C(1)N(1)C(2)	175.1(2)	S(7)C(24)N(5)C(25)	–179.2(2)	S(2)Zn(1)N(3)C(11)	–74.6(2)	S(5)Zn(2)N(6)C(29)	–66.9(2)
S(1)C(1)N(1)C(4)	–2.1(3)	S(7)C(24)N(5)C(27)	4.2(3)	S(2)Zn(1)N(3)C(15)	154.6(1)	S(5)Zn(2)N(6)C(33)	166.5(1)
S(2)C(1)N(1)C(2)	–5.7(3)	S(8)C(24)N(5)C(25)	0.0(3)	S(3)Zn(1)N(3)C(11)	123.9(2)	S(8)Zn(2)N(6)C(29)	120.9(2)
S(2)C(1)N(1)C(4)	177.1(2)	S(8)C(24)N(5)C(27)	–176.6(2)	S(3)Zn(1)N(3)C(15)	–6.9(2)	S(8)Zn(2)N(6)C(33)	–5.7(2)
S(3)C(6)N(2)C(7)	176.8(2)	S(5)C(19)N(4)C(22)	176.9(2)	S(4)Zn(1)N(3)C(11)	43.6(2)	S(7)Zn(2)N(6)C(29)	47.0(2)
S(3)C(6)N(2)C(9)	–3.2(3)	S(5)C(19)N(4)C(20)	–0.6(3)	S(4)Zn(1)N(3)C(15)	–87.2(2)	S(7)Zn(2)N(6)C(33)	–79.6(1)

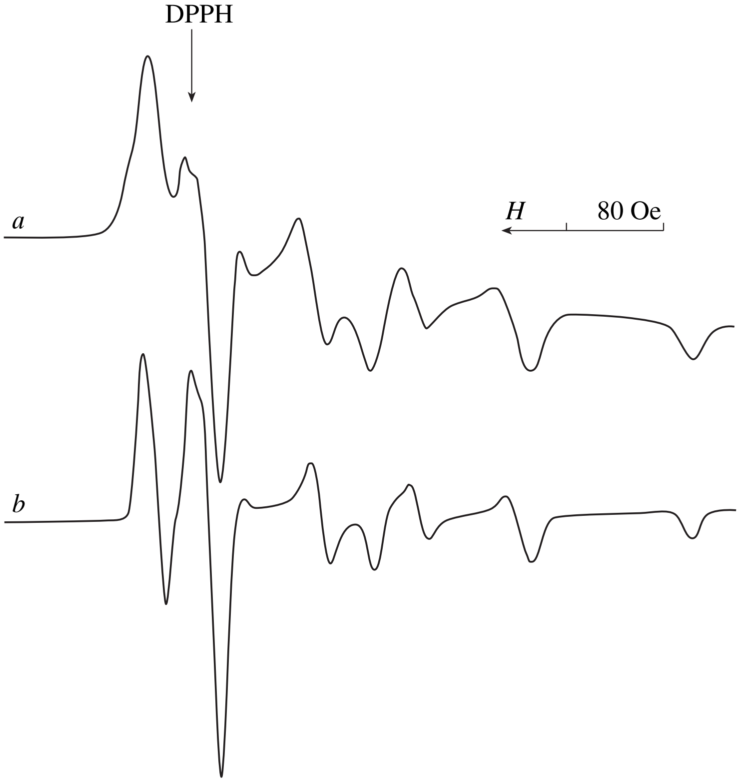

Fig. 1. (*a*) Experimental and (*b*) model EPR spectra of the adduct $[^{63}Cu\{NH(C_4H_9)_2\}\{S_2CN(CH_3)_2\}_2]$ magnetically diluted with zinc(II).

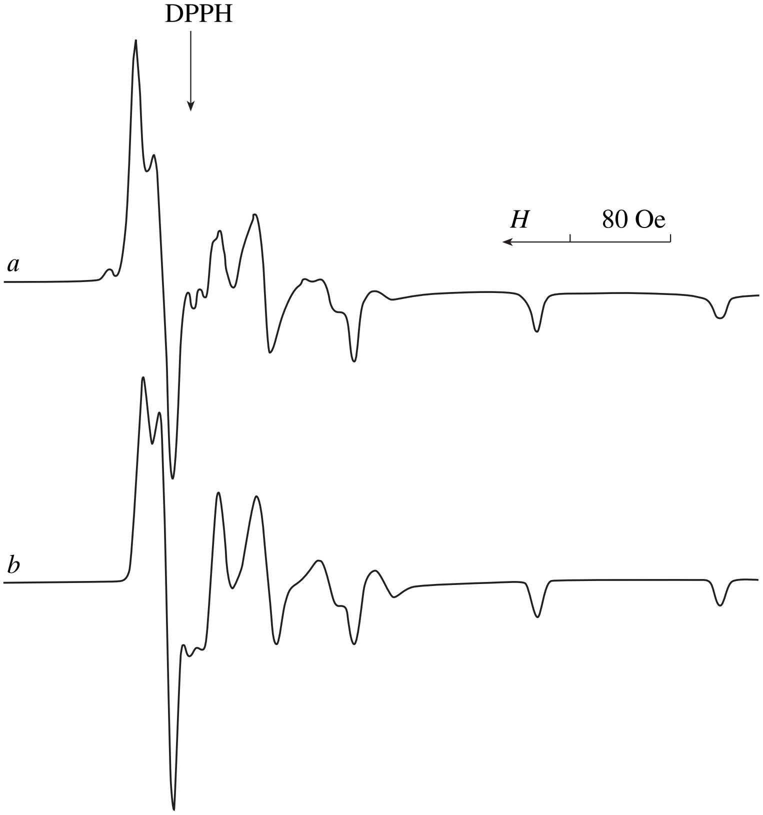

Fig. 2. (*a*) Experimental and (*b*) model EPR spectra of the adduct $[^{63}Cu\{NH(i\text{-}C_4H_9)_2\}\{S_2CN(C_2H_5)_2\}_2]$ magnetically diluted with zinc(II).

Table 4. EPR parameters of the adducts of copper(II) dialkyldithiocarbamates*

Complex	g_1	A_1^{Cu}, Oe	g_2	A_2^{Cu}, Oe	g_3	A_3^{Cu}, Oe
$[Cu\{NH(C_4H_9)_2\}\{S_2CN(CH_3)_2\}_2]$ (VI)	2.117	111/119	2.078	69/74	2.008	19/20
$[Cu\{NH(C_4H_9)_2\}\{S_2CN(C_2H_5)_2\}_2]$ (VII)	2.106	103/110	2.094	77/82	2.006	46/49
$[Cu\{NH(C_4H_9)_2\}\{S_2CN(CH_2)_4O\}_2]$ (VIII)	2.123	126/135	2.026	12/13	2.041	12/13
$[Cu\{NH(i\text{-}C_4H_9)_2\}\{S_2CN(CH_3)_2\}_2]$ (IX)	2.129	130/139	2.049	53/57	2.009	16/17
$[Cu\{NH(i\text{-}C_4H_9)_2\}\{S_2CN(C_2H_5)_2\}_2]$ (X)	2.121	132/141	2.051	43/46	2.023	24/26

* The HFS constants are given for the $^{63}Cu/^{65}Cu$ nuclides.

^{15}N nucleus (**I** = 1) under the given conditions of MAS experiments [20, 21]. The exceptions are adducts **IV** and **V**; their ^{13}C NMR spectra contain a singlet and a 1 : 1 : 1 : 1 quartet (Figs. 3a, 3b). The foregoing spectral patterns partially correlate with ^{15}N NMR spectra (Table 5) showing 1 : 1 doublets (for **I–III**) and a 1 : 1 : 1 : 1 quartet (for **V**) in the range of Dtc resonance signals (Fig. 4). In addition, the ^{15}N NMR spectra contain one (for **I–IV**) or two signals (for **V**) due to the coordinated bases. Thus, the ^{13}C and ^{15}N MAS NMR data suggest that crystalline adducts **I–IV** exist as single molecules, while $[Zn\{NH(i\text{-}C_4H_9)_2\}\{S_2CN(C_2H_5)_2\}_2]$ (**V**) exists as two isomeric molecules. In all the adducts, the Dtc ligands are structurally nonequivalent. Structural differences between the isomeric molecules in adduct **V** were revealed by X-ray diffraction analysis.

Molecular structure of adduct V. The unit cell of adduct **V** includes eight $[Zn\{NH(i\text{-}C_4H_9)_2\}\{S_2CN(C_2H_5)_2\}_2]$ molecules. Four of them are structurally nonequivalent with the other four (Fig. 5; Table 3). In each molecule, the Zn atom in the chromophore $[ZnNS_4]$ coordinates a diisobutylamine molecule and two Dtc ligands, showing C.N. 5. The zinc polyhedron is intermediate between TP and TBP. In the equatorial plane of TBP, the zinc atom coordinates the N atom of diisobutylamine and two S atoms of the Dtc ligands (via shorter Zn–S bonds). The two other, more distant S atoms are in the axial positions. In [22], the parameter $\tau = (\alpha - \beta)/60$ was proposed for quantitative characterization of the polyhedra in complexes of metals with C.N. 5; α and β are the largest two SZnS angles ($\alpha > \beta$). For an idealized TP (C_{4v}) τ is zero because

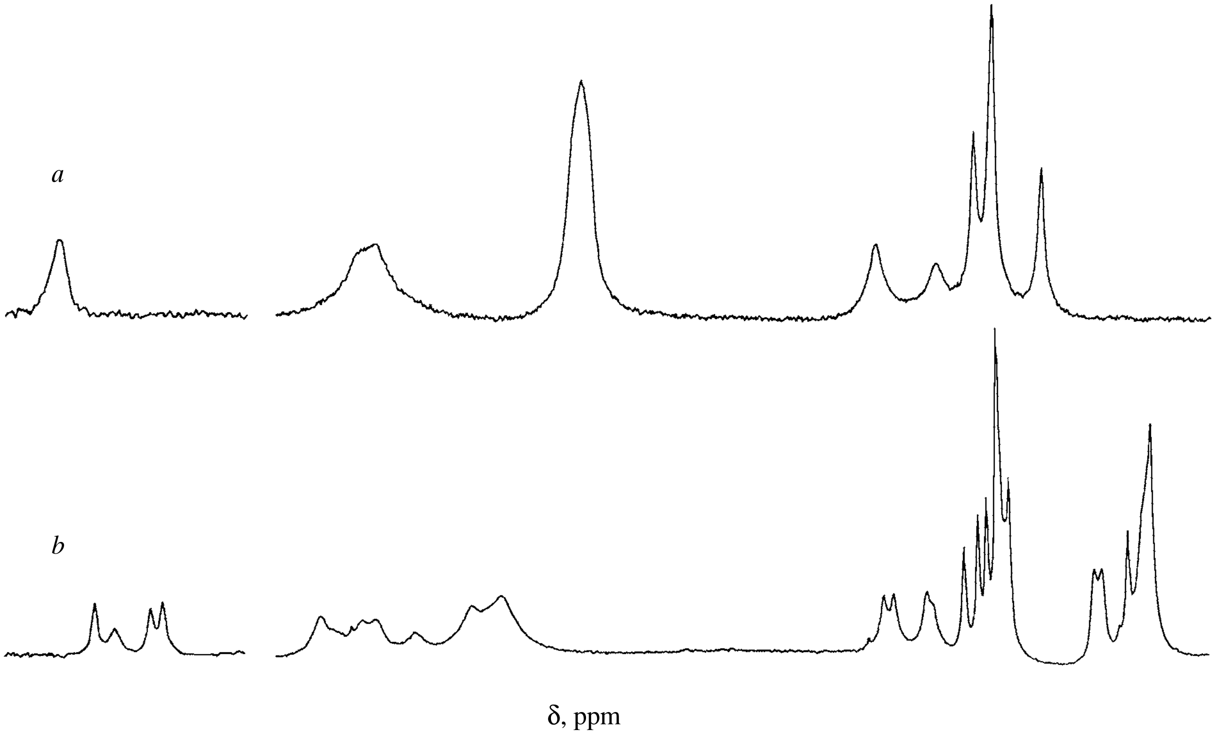

Fig. 3. ^{13}C MAS NMR spectra of the crystalline adducts $[Zn\{NH(i\text{-}C_4H_9)_2\}(S_2CNR_2)_2]$ for R = (*a*) CH_3 and (*b*) C_2H_5; the number of scans/spinning frequency (Hz) is (*a*) 1820/5000 and (*b*) 1520/5000.

Table 5. ^{13}C and ^{15}N chemical shifts δ (ppm) for the adducts with reference to TMS and NH_4Cl, respectively

Complex	$^{-}$S(S)CNR$_2$ (R = CH_3, C_2H_5; R_2 = $(CH_2)_4O$)					NHR$'_2$ (R' = C_4H_9, i-C_4H_9)				
	–S(S)CN=	=N–CH$_2$–	–CH$_3$	–CH$_2$–O–	=N–	=N–CH$_2$–	–CH$_2$–	–CH–	–CH$_3$	=N–
$[\mathrm{Zn}\{\mathrm{NH}(\mathrm{C_4H_9})_2\}\{\mathrm{S_2CN}(\mathrm{CH_3})_2\}_2]$ (I)	206.9 (47)* 205.9 (51)* (1 : 1)		47.0 (45)* 46.3, 45.5 (1 : 1 : 2)		105.0 101.7 (1 : 1)	52.5 49.8 (1 : 1)	32.1, 30.7 (1 : 1) 22.1, 21.9 (1 : 1)		16.5 14.9 (1 : 1)	9.7
$[\mathrm{Zn}\{\mathrm{NH}(\mathrm{C_4H_9})_2\}\{\mathrm{S_2CN}(\mathrm{C_2H_5})_2\}_2]$ (II)	204.3 (46)* 203.5 (51)* (1 : 1)	48.6	12.9, 12.8 12.2 (1 : 2 : 1)		134.2 130.7 (1 : 1)	50.5	30.7, 29.5 21.3 (1 : 1 : 2)		16.8 15.4 (1 : 1)	–0.9
$[\mathrm{Zn}\{\mathrm{NH}(\mathrm{C_4H_9})_2\}\{\mathrm{S_2CN}(\mathrm{CH_2})_4\mathrm{O}\}_2]$ (III)	204.9 204.2 (1 : 1)	51.9		67.7 66.6 (1 : 1)		54.7	32.7, 31.8 (1 : 1) 22.4, 21.4 (1 : 1)		15.0	
$[\mathrm{Zn}\{\mathrm{NH}(i\text{-}\mathrm{C_4H_9})_2\}\{\mathrm{S_2CN}(\mathrm{CH_3})_2\}_2]$ (IV)	207.0 (35)*		46.3 45.8 45.4 (1 : 2 : 1)		101.4 100.0 (1 : 1)	58.7 57.6 (1 : 1)		28.7 25.2 (1 : 1)	23.1, 22.1 19.2 (1 : 2 : 1)	–2.0
$[\mathrm{Zn}\{\mathrm{NH}(i\text{-}\mathrm{C_4H_9})_2\}\{\mathrm{S_2CN}(\mathrm{C_2H_5})_2\}_2]$ (V)	205.3 204.5 203.1 202.7 (1 : 1 : 1 : 1)	55.3 52.0 50.2 (1 : 2 : 5)	16.1, 15.7 14.2, 13.4 13.0, 12.8 (1 : 1 : 1 : 1 : 1 : 3)		134.2 133.8 130.4 129.8 (1 : 1 : 1 : 1)	60.8 58.3 57.6 (2 : 1 : 1)		28.3, 27.7 25.8, 25.4 (1 : 1 : 1 : 1)	23.6, 22.8 22.3, 21.8 21.6, 21.0 (1 : 1 : 1 : 2 : 2 : 1)	–0.6 –2.6 (1 : 1)

* The asymmetric ^{13}C–^{14}N doublets (Hz).

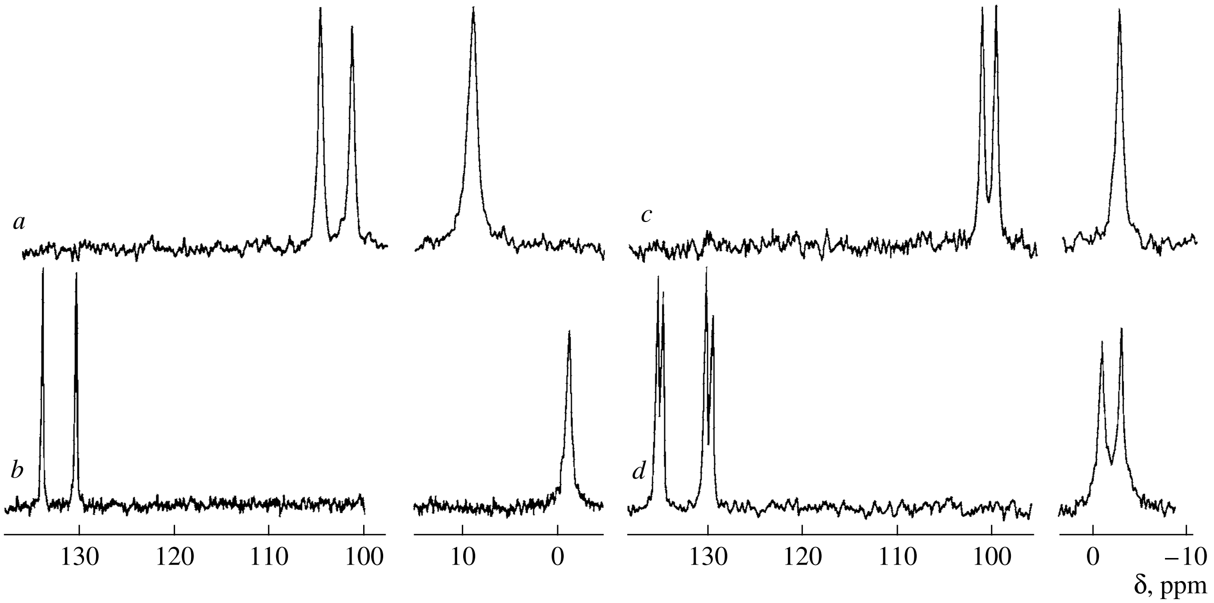

Fig. 4. ^{15}N MAS NMR spectra of the adducts $[Zn(NHR'_2)(S_2CNR_2)_2]$ for R' = (*a*, *b*) C_4H_9 and (*c*, *d*) *i*-C_4H_9 and R = (*a*, *c*) CH_3 and (*b*, *d*) C_2H_5; the number of scans/spinning frequency (Hz) is (*a*) 4000/3000, (*b*) 3080/3000, (*c*) 3620/3000, and (*d*) 7600/2800.

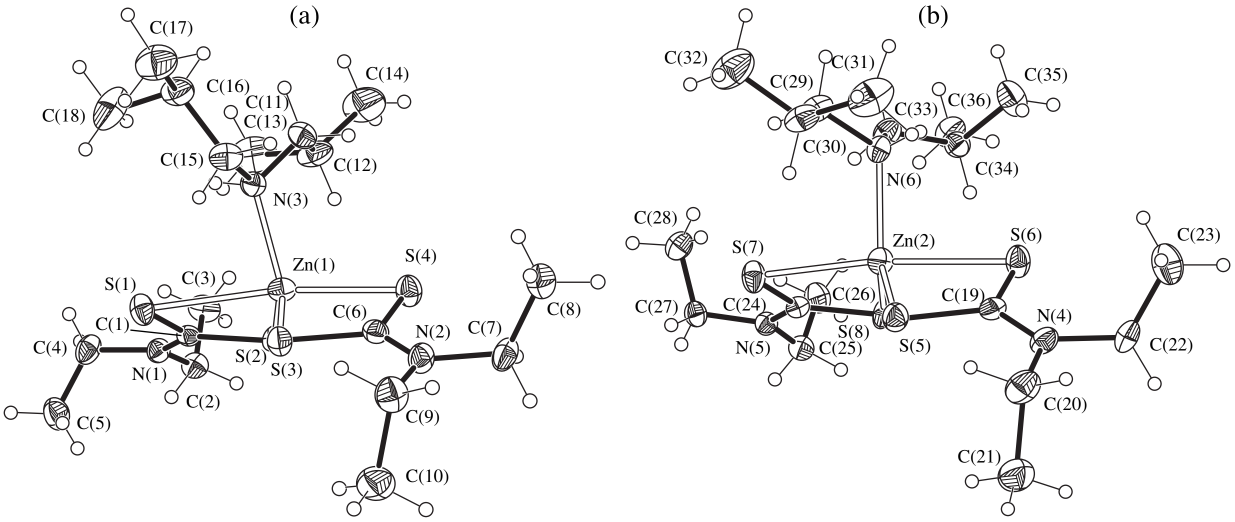

Fig. 5. Molecular structures of the conformers (a*)* **A** and (b) **B** of $[Zn\{NH(i\text{-}C_4H_9)_2\}\{S_2CN(C_2H_5)_2\}_2]$ with atomic thermal displacement ellipsoids (50% probability).

$\alpha = \beta$. In a regular TBP (C_{3v}), the axial SZnS angle (α) is 180°, while the equatorial angle (β) is 120°; i.e., $\tau = 1$. Any distorted polyhedron is described by $0 < \tau < 1$. According to our calculations, the contribution from TBP to one molecule (with Zn(1)) is slightly lower (68.8%) than to the other (with Zn(2), 74.2%).

S,S'-Anisobidentate coordination of the Dtc ligands (in all adducts, one Zn–S bond is substantially shorter than the other) gives rise to small four-membered chelate rings [ZnSSC] with fairly short Zn···C/S···S distances: 2.802/2.953 and 2.954/2.972 Å (Zn(1)) and 2.864/2.951 and 2.877/2.955 Å (Zn(2)). The chelate rings is not absolutely planar because of the folding along the S–S bond: the dihedral angles between the planes of the [ZnSS] and [CSS] fragments are 171.49° and −176.75° (Zn(1)) and −172.68° and −173.69° (Zn(2)). Such a configuration of the four-membered chelate ring is favorable for the *trans*-annular effect to appear. The N–C(S)S bonds are stronger than the N–CH_2 bonds and reflect the contribution of double bonding to the formally single bond (because the *sp*^{2}-hybridized N atom undergoes partial *sp*^{3}-hybridization). That is why the $C_2NC(S)S$ fragments are virtually planar, although the C(2) and C(27) atoms in two of them slightly deviate from the plane (Table 3).

The structural similarity of the adduct molecules allows them to be classified as conformers, when a polyatomic molecular system reaches equilibrium in two or more configurations with close energies. Note the essential distinctions between conformers **A** (Zn(1)) and **B** (Zn(2)) (Table 3):

—the Zn–N bond in conformer **A** (2.084 Å) is stronger than in conformer **B** (2.104 Å);

—conformer **A** contains the Dtc ligands with the most (the S(1) and S(2) atoms) and least pronounced anisobidentate character (the S(3) and S(4) atoms) of coordination;

—the axial Zn–S bonds in the Zn(2) polyhedron are virtually equal, while their lengths for Zn(1) differ by 0.34 Å and its polyhedron combines the strongest and weakest $Zn–S_{ax}$ bonds;

—the contributions from TBP (TP) to the geometry of the zinc polyhedron in conformers **A** and **B** are 68.8% (31.2%) and 74.2% (25.8%), respectively;

—the coordinated diisobutylamine molecules in conformers **A** and **B** differ in spatial orientation, which is quantitatively expressed in terms of the torsion angles SZnNC (Table 3). The orientations of these molecules relative to the strongest equatorial bonds (Zn(1)–S(2) and Zn(2)–S(5)) differ on average by ~10°.

The manifestation of conformational isomerism in adduct **V** only can be explained by the steric effect of two bulky alkyl substituents in diisobutylamine.

Assignment of NMR signals. Let us consider possible assignments of ^{13}C and ^{15}N NMR signals to the atomic positions in the crystallographically independent conformers of adduct **V**. The different N–C(S)S bond lengths in four Dtc ligands indicate different contributions of double bonding (or, what is the same thing, different degrees of mixing of the *sp*^{2}- with *sp*^{3}-hybridization states of the N and C atoms) [4, 23]. The greater contribution of the *sp*^{2}-hybridization state will correspond to the stronger bond. In terms of the mesomeric effect, this causes the electron density to shift toward the –C(S)S– fragment, thus increasing the charge δ^+ on the N atom. This can be schematically represented as follows:

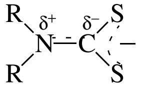

As the result, the N nucleus is less shielded by electrons, while the C nucleus is more shielded. Thus, the shorter the N–C(S)S bond, the higher the charges δ^+ and δ^- on the N and C atoms and, consequently, the higher the ^{15}N chemical shifts and the lower the ^{13}C chemical shifts for these atoms [4]:

Bond	N(1)–C(1)	N(5)–C(24)	N(4)–C(19)	N(2)–C(6)
d, Å	1.336	1.332	1.329	1.328
δ ^{15}N, ppm	129.8	130.4	133.8	134.2
δ ^{13}C, ppm	205.3	204.5	203.1	202.7

When assigning ^{15}N NMR signals for coordinated diisobutylamine molecules, the character (different strengths) of their coordination should be taken into account. Since nitrogen is more electronegative than zinc, the electron density of the Zn–N bond will be shifted to the N atom, thus increasing the shielding of its nucleus. This effect will be more pronounced for the stronger Zn–N bond. Thus, the ^{15}N NMR signal at lower δ (–2.6 ppm) should be assigned to the N(3) atom of the more strongly bonded amine (in conformer **A**), while the signal at $\delta = -0.6$ ppm is due to the N(6) atom in conformer **B**.

ACKNOWLEDGMENTS

The authors are grateful to the research engineer M. Ranheimer for her constant assistance and to the Bruker Co. for free access to the WIN-EPR SimFonia program.

This work was supported by the Russian Foundation for Basic Research and the Far East Division of the Russian Academy of Sciences (Program “Dal’nii Vostok”, grant no. 06-03-96009) and the Presidium of the Far East Division of the Russian Academy of Sciences (grant no. 05-III-G-04-060 on Basic and Applied Researches by Young Scientists, 2005).

A.V. Ivanov acknowledges the financial support of the Agricola Research Center at the Luléa University of Technology (Sweden).

REFERENCES

1. O’Brien, P., *Inorganic Materials*, Bruce, D.W. and O’Hare, D., Eds., New York: Wiley, 1992.
2. Ivanov, A.V., Mitrofanova, V.I., Kritikos, M., and Antzutkin, O.N., *Polyhedron*, 1999, vol. 18, no. 15, p. 2069.
3. Ivanov, A.V. and Antzutkin, O.N., *Polyhedron*, 2002, vol. 21, nos. 27–28, p. 2727.
4. Ivanov, A.V. and Antzutkin, O.N., *Topics in Current Chem.*, 2005, vol. 246, p. 271.
5. Ivanov, A.V., Mitrofanova, V.I., Rodina, T.A., and Mel’nipkova, M.A., *Koord. Khim.*, 1997, vol. 23, no. 11, p. 838.
6. Ivanov, A.V., Forsling, W., Kritikos, M., et al., *Dokl. Akad. Nauk*, 1999, vol. 369, no. 1, p. 64.
7. Ivanov, A.V., Kritikos, M., Antzutkin, O.N., and Forsling, W., *Inorg. Chim. Acta,* 2001, vol. 321, nos. 1–2, p. 63.
8. Ivanov, A.V., Ivakhnenko, E.V., Gerasimenko, A.V., and Forsling, V., *Zh. Neorg. Khim.*, 2003, vol. 48, no. 1, p. 52 [*Russ. J. Inorg. Chem.* (Engl. Transl.), vol. 48, no. 1, p. 45].

9. Pines, A., Gibby, M.G., and Waugh, J.S., *J. Chem. Phys.*, 1972, vol. 56, no. 4, p. 1776.
10. Earl, W.L. and VanderHart, D.L., *J. Magn. Reson.*, 1982, vol. 48, no. 1, p. 35.
11. Ratcliffe, C.I., Ripmeester, J.A., and Tse, J.S., *Chem. Phys. Lett.*, 1983, vol. 99, no. 2, p. 177.
12. Mason, J, in *Encyclopedia of Nuclear Magnetic Resonance*, Grant, D.M. and Harris, R.K., Eds., New York: Wiley, 1996, vol. 5, p. 3222.
13. *SMART and SAINT-Plus. Versions 5.0. Data Collection and Processing Software for the SMART System,* Madison (WI, USA): Bruker AXS, 1998.
14. *SHELXTL/PC. Versions 5.10. An Integrated System for Solving, Refining and Displaying Crystal Structures from Diffraction Data*, Madison (WI, USA): Bruker AXS, 1998.
15. Ovchinnikov, I.V. and Konstantinov, V.N., *J. Magn. Reson.*, 1978, vol. 32, no. 2, p. 179.
16. Rieger, Ph.H., *Electron Spin Resonance (Senior Reporter Symons M.C.R.)*, vol. 13B, Newcastle upon Tyne: Athenaeum Press Ltd., 1993, p. 178.
17. Arriortua, M.A., Mesa, J.L., Rojo, T., et al., *Inorg. Chem.*, 1988, vol. 27, no. 17, p. 2976.
18. Murakami, T., Takei, T., and Ishikawa, Y., *Polyhedron*, 1997, vol. 16, no. 1, p. 89.
19. Ivanov, A.V., Forsling, W., Antzutkin, O.N., and Novikova, E.V., *Koord. Khim.*, 2001, vol. 27, no. 3, p. 174.
20. Hexem, J.G., Frey, M.H., and Opella, S.J., *J. Chem. Phys.*, 1982, vol. 77, no. 7, p. 3847.
21. Harris, R.K., Jonsen, P., and Packer, K.J., *Magn. Reson. Chem.*, 1985, vol. 23, no. 7, p. 565.
22. Addison, A.W., Rao, T.N., Reedijk, J., et al., J. *Chem. Soc., Dalton Trans.*, 1984, no. 7, p. 1349.
23. Higgins, G.M.C. and Saville, B., *J. Chem. Soc.,* 1963, no. 3, p. 2812.